2019-04-04

Localised anthropogenic wake generates a predictable foraging hotspot for top predators

Lieber, L

1 # Localised anthropogenic wake generates a predictable foraging hotspot
2 # for top predators

3

4 Lilian Lieber[1,], W. Alex M. Nimmo-Smith[2], James J. Waggitt[3], Louise Kregting[1]

5 [1] School of Natural and Built Environment, Queen's University Marine Laboratory, 12-13 The Strand, Portaferry
6 BT22 1PF, Northern Ireland, UK
7 [2] Marine Institute, University of Plymouth, Drake Circus, Plymouth PL4 8AA, England, UK
8 [3] School of Ocean Sciences, Bangor University, Menai Bridge, Anglesey, LL59 5AB, Wales, UK
9
10 *Corresponding author.
11 E-mail address: l.lieber@qub.ac.uk

12

13 **Abstract**

14 With rapid expansion of offshore renewables, a broader perspective on their ecological implications

15 is timely to predict marine predator responses to environmental change. Strong currents interacting

16 with man-made structures can generate complex three-dimensional wakes that can make prey more

17 accessible. Whether localised wakes from man-made structures can generate predictable foraging

18 hotspots for top predators is unknown. Here we address this question by quantifying the relative use

19 of an anthropogenically-generated wake by surface foraging seabirds, verified using drone transects

20 and hydroacoustics. We show that the wake of a tidal energy structure promotes a localised and

21 persistent foraging hotspot, with seabird numbers greatly exceeding those at adjacent natural wake

22 features. The wake mixes material throughout the water column, potentially acting like a prey

23 conveyer belt. Our findings highlight the importance of identifying the physical scales and

24 mechanisms underlying predator hotspot formation when assessing the ecological consequences of

25 installing or removing anthropogenic structures.

26

27

28

29

30   In an era of intense marine urbanisation[1], understanding scale-dependent physical forcing can help

31   predict how marine predators may respond to environmental change. Predators rely on a multitude

32   of physical processes which dynamically influence foraging behaviour[2,3] and success[4]. In the open

33   ocean, predator foraging has been associated with mesoscale (10 – 100 km) physical features, such

34   as fronts and eddies[5,6,7]. However, even fine- (<1 km, e.g. internal waves[3]) or local- (10 –100 m, e.g.

35   island wakes[8]) scale physical features may create small-scale predator hotspots[9,10]. The importance

36   of these fine and local-scale physical processes is heightened in seabirds restricted to shallow plunge

37   diving techniques, such as gulls and terns, where prey availability near the sea surface governs

38   foraging site selection[11,12,13]. Consequently, tern species (*Sternidae*) tend to focus their foraging

39   activity in areas of bathymetry-generated turbulence or shallow upwellings that consistently make

40   prey available near the surface[11, 12,14,15]. Such physically-enhanced prey availability and its

41   predictability seem to determine seabird foraging habitat rather than prey density alone[12,16,17, 18,19,20].

42   Therefore, the identification of local flow processes interacting with bathymetric features (natural or

43   man-made) can improve our understanding of the physical mechanisms promoting foraging hotspot

44   formation and persistence in dynamic coastal systems[21].

45   The periodic emergence of tidally-driven bathymetry-induced turbulence, shallow

46   upwellings or more ephemeral turbulent structures such as boils - circular regions of local

47   upwelling[22] - are characteristic of strongly tidal seas. The introduction of anthropogenic structures

48   into such dynamic environments adds further complexity to local flow processes, potentially

49   triggering ecological implications[23]. Man-made structures modify local hydrodynamics[24], including

50   flow velocities[25] and wake effects[26,27,28]. Further, a von Kármán vortex street[29], characterised by

51   distinct and repeatable eddy trajectories, may occur in the wake of embedded structures when

52   placed in strong, near-laminar flows[30]. While fish may exploit the lee of a structure as a flow refuge[31]

53   or use small-scale vortices (e.g. <1:1 ratio of vortex to fish size) to Kármán gait[32], an extreme

54   downstream wake with eddy vortices of sufficient size and vorticity[33] can vertically displace or

55   overturn fish in fast, unsteady flows[31,34,35, 36], potentially making them accessible to surface-foraging

56   predators.

57   We hypothesised that a vortex street attributable to a man-made structure could present an

58   as yet unexplored mechanism for localised predator hotspot formation. Here, we investigate

59   whether an anthropogenically-generated wake can present a reliable foraging location for surface-

60   feeding seabirds (*Sternidae*), comparable to those at adjacent natural wake features. SeaGen, the

61   world's first grid-connected tidal energy turbine, currently being decommissioned, produces a wake

62   with vortex shedding approaching a von Kármán vortex street[30]. The device consisted of a monopile

63   structure (3 m diameter) attached to a quadropod foundation fixed on the seabed (water depth

64   about 25 m) with a 27 m long crossbeam supporting the original rotors on either side of the tower

65   15 m above the seabed. During this study, the rotors had already been removed, however the

66   monopile itself contributes considerably to the vortex shedding in the downstream wake as shown

67   through large eddy simulations[30]. SeaGen is situated in a dynamic tidal channel ('the Narrows') in

68   Strangford Lough, Northern Ireland, in proximity to colonies of summer-breeding tern species

69   (*Sterna hirundo, S. sandvicensis, S. paradisaea*). The channel also provides diverse foraging

70   opportunities with natural wake features commonly used by terns, therefore presenting a suitable

71   study system. Two neighbouring extreme natural wake features, an island (Walter's Rock) and a

72   whirlpool structure (Routen Wheel), within the channel were selected to compare the terns' use of

73   the natural wakes with the man-made wake (Fig. 1). Our findings show that among all three wake

74   features investigated, the flood wake associated with the man-made structure promotes the most

75   persistent and intense foraging aggregations of terns. We further provide evidence that foraging

76   over the wake is highly localised, highlighting the importance and ecological implications of localised

77   physical forcing around man-made structures.
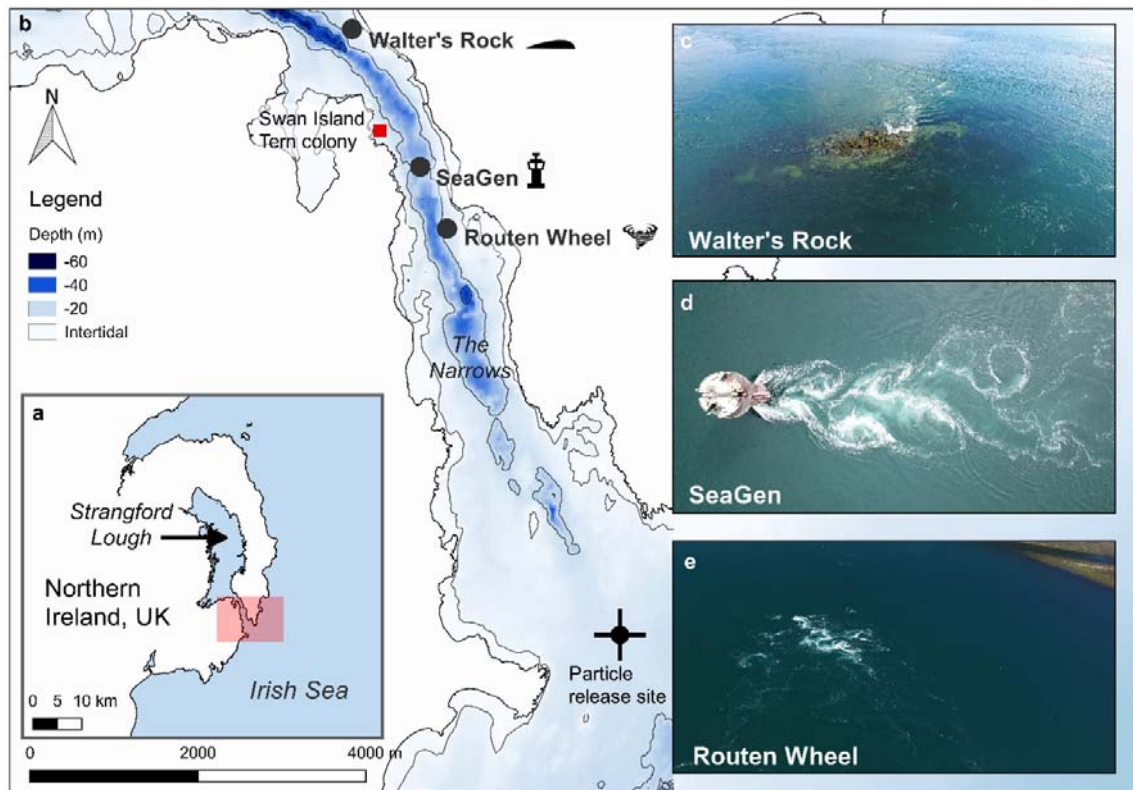
Fig. 1: **Location of wake features in the Narrows tidal channel situated in Strangford Lough, Northern Ireland, UK. a**, Overview map showing the study area within the Narrows, highlighted by a red box. **b**, Location of wake features in the Narrows. **c-e**, Insets showing the turbulent structures associated with each wake feature. Note: particle release site indicates the release of passive particles (as a proxy for prey organisms) from the Irish Sea during flood tide within a hydrodynamic model.

Results

Tern foraging patterns vary among wake features The number of terns foraging at each wake

feature was assessed using vantage point surveys (Jul-Aug 2018) with observations covering

different tidal states (ebb versus flood, spring versus neap), recording variations in tern abundance

across hydrodynamic conditions. The occurrence of conspicuous topographic and anthropogenic

landmarks allowed the construction of plots with approximately the same area, with calculations

based on bearings and distances from the vantage point. For SeaGen, observations were spatially

divided into North (area of flood tide wake) and South (area of ebb tide wake) of the foundation,

respectively. While the physical structure of SeaGen's wake does not differ between the flood and

ebb tide, the spatial separation was needed to ensure equal spatial extent per site. Further, it helped

94   to assess whether terns were solely attracted to the environmental cue of turbulence ('ecological

95   trap'[37]) or if aggregations were coupled to the ebb-flood tidal cycle.
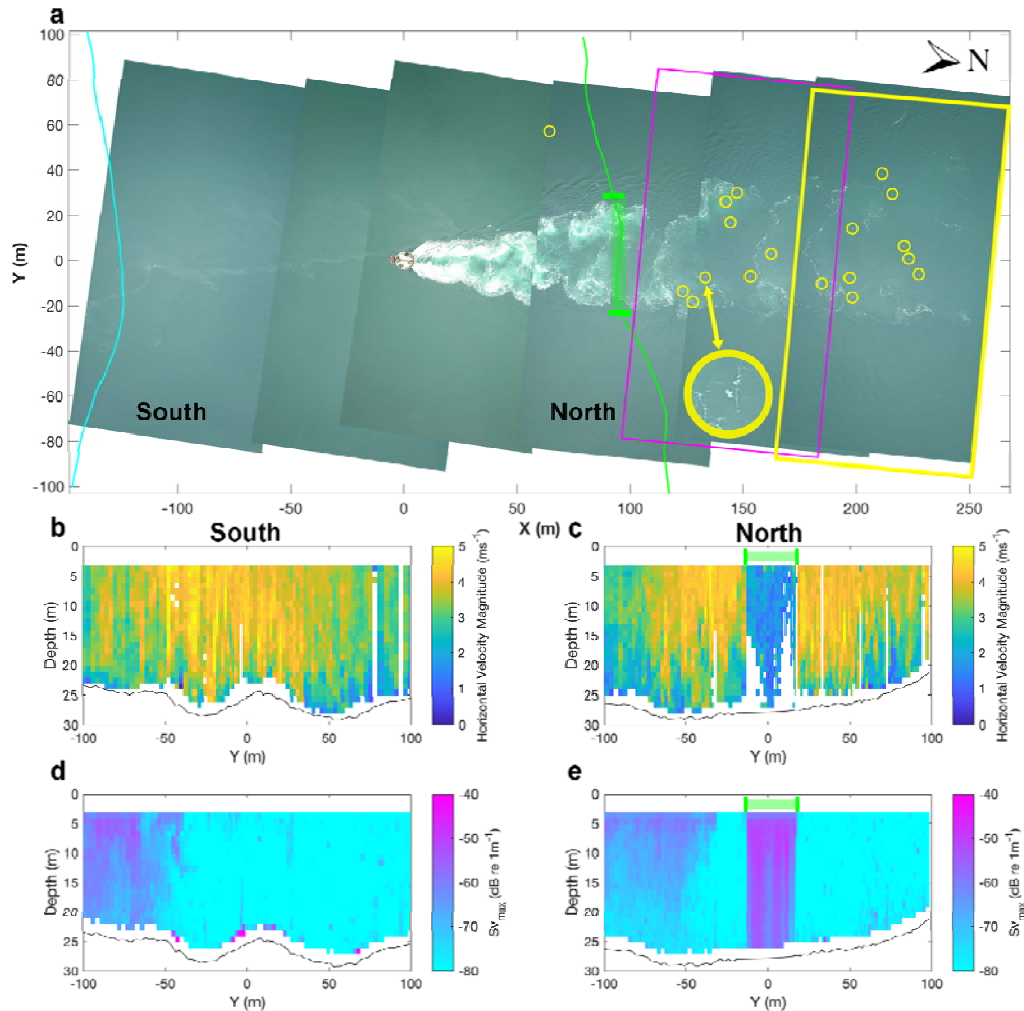
96   Tidal coupling was evident with the highest probability of encountering terns at SeaGen

97   North and Walter's Rock during flood tides, and Routen Wheel during ebb tides (Fig. 2a & b). The

98   largest flocks of terns were encountered at SeaGen North during peak flood tides (Fig. 2c), with

99   aggregations frequently exceeding 50 birds (Fig. 2a). On average, tern numbers observed foraging at

100   the SeaGen North site during peak flood were three times as many as those foraging at either of the

101   two natural wake sites (Fig. 2c). Because of high overdispersion and zero-inflation in the datasets, a

102   hurdle-model was used to divide statistical analysis into presence-absence and count components[38].

103   In summary, the mean probability of encountering terns and number of terns if encountered per

104   minute differed significantly among the wake features (Table 1). There were significant variations in

105   probabilities of encountering terns and numbers of terns if encountered (Fig. 2 a &b) across tidal

106   states at most locations (an exception to this was SeaGen South).
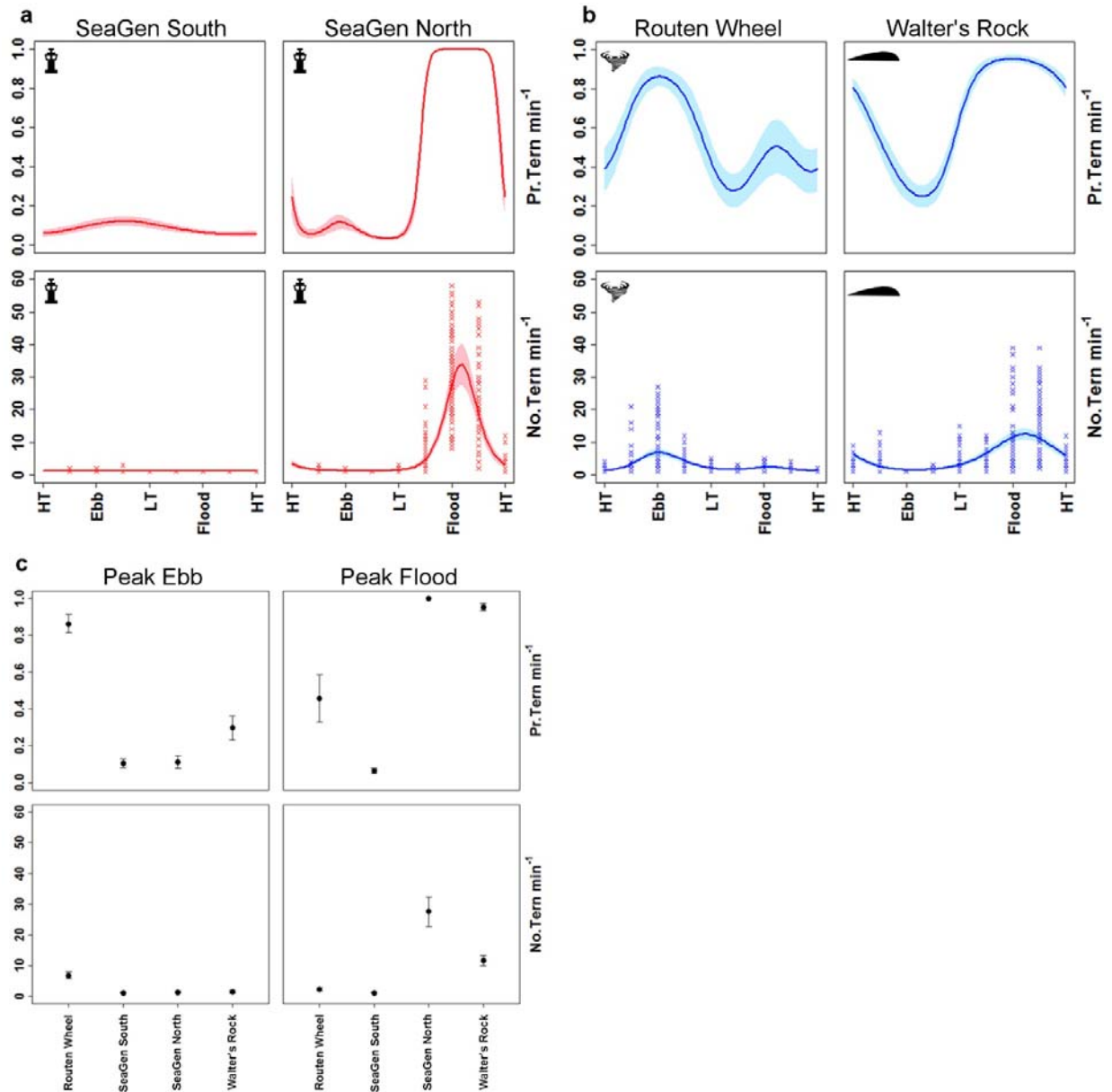
Fig. 2: Tern counts over tidal state at each wake feature. **a & b,** Mean ±SE variations in the predicted probability of encountering terns and the number of terns if encountered per minute across tidal states around SeaGen North and South (**a**), the Routen Wheel and Walter's Rock (**b**) wake features, respectively. Crosses indicate the recorded number of terns if encountered binned into periods representing eight different states (1hr 20min) of the ebb-flood cycle. HT= High tide, LT=Low tide. **c**, Mean ±SE variations in the predicted probability of encountering terns and the number of terns if encountered per minute across tidal states and locations. Tidal states represent peak current speeds in ebb and flood directions. All predictions (**a**-**c**) were made using model parameters from a general-additive mixed effect model (GAMM) with significance in both probabilities and numbers across tidal states shown in Table 1.

Tern foraging in relation to man-made wake Overall, the probability and size of tern aggregations was highest at the man-made structure (SeaGen North), triggering a fine-scale investigation of its wake dynamics. Unmanned aerial vehicle (UAV) transects above SeaGen over several tidal cycles visualised the dynamic vortex shedding of the wake and the exact spatial extent of tern foraging,

121   thereby overcoming the oblique angle of the vantage point observer. Consistent with the vantage

122   point surveys, these transects recorded that terns focused their foraging activity almost exclusively

123   over the flood wake (SeaGen North; Fig. 3a). The lee wake vortices showed the distinct and

124   predictable pattern consistent with a von Kármán vortex street, with a surface-tracked eddy

125   shedding frequency of 10 - 14 min^{-1}.

126

127   **Fig. 3: Tern distribution during peak flood tide in relation to SeaGen's wake structure. a**, Georeferenced

128   composite panoramic image from UAV transect survey with terns identified (yellow circles – one enlarged for

129   clarity). The orientation of the x-axis is 349 degrees. Magenta and yellow boxes indicate tracking regions

130   shown in Figure 4. **b-c**, Horizontal velocity magnitude (ms^{-1}) profile from the southern (cyan) and northern

131   (green) ADCP transect, respectively. **d-e**, Maximum acoustic backscatter (dB re 1m^{-1}) profile from the southern

132   and northern ADCP transect, respectively. The North transects show a clear water column velocity deficit (**c**)

133   and backscatter (an indicator for macro-turbulence) signature (**e**) in the area of the flood wake (Y=-20–20m).

134   To assess vertical wake effects throughout the water column, vessel-mounted acoustic

135   Doppler current profiler (ADCP) transects were run either side of the SeaGen foundation throughout

136   a flood-ebb tidal cycle. The upstream near-laminar flow exceeding 5 ms^{-1} experiences a clear velocity

137   deficit downstream in the midline of the structure throughout the water column with a cross-stream

138   extent of 45 m at approximately 100 m downstream of SeaGen (Fig. 3b, c). The corresponding

139   signature of elevated acoustic backscatter, an indicator for macro-turbulence[39], visible in the

140   downstream wake (Fig. 3e) is most likely dominated by entrained bubbles[40], and to a lesser extent,

141   sediment re-suspension[41] and perhaps fish[42,43]. Bounded by the sea surface and seafloor, the

142   backscatter signature from the wake of the structure is distinct from adjacent water. This provides

143   evidence that the turbulent eddies within the flow are powerful enough to up-and down-well

144   submerged material throughout the entire water column. While extreme water column scattering

145   from bubbles and sediment precludes the acoustic extraction of fish targets from turbulence, the

146   wake likely has the potential to act as a prey "conveyor belt" for surface foragers.

147   Applying machine learning algorithms to distinguish terns from other moving targets (e.g.

148   foam), flight trajectories recorded over the wake region (Fig. 4a) showed a high degree of in-flight

149   sinuosity, typical for area-restricted search behaviour in response to increased prey intake

150   rate/profitability (characterised by decreased flight speeds and frequent turning[2], Fig. 4b). The terns

151   forage almost exclusively over the vortex street with mostly transit flights to and from the colony

152   outside of this central region.
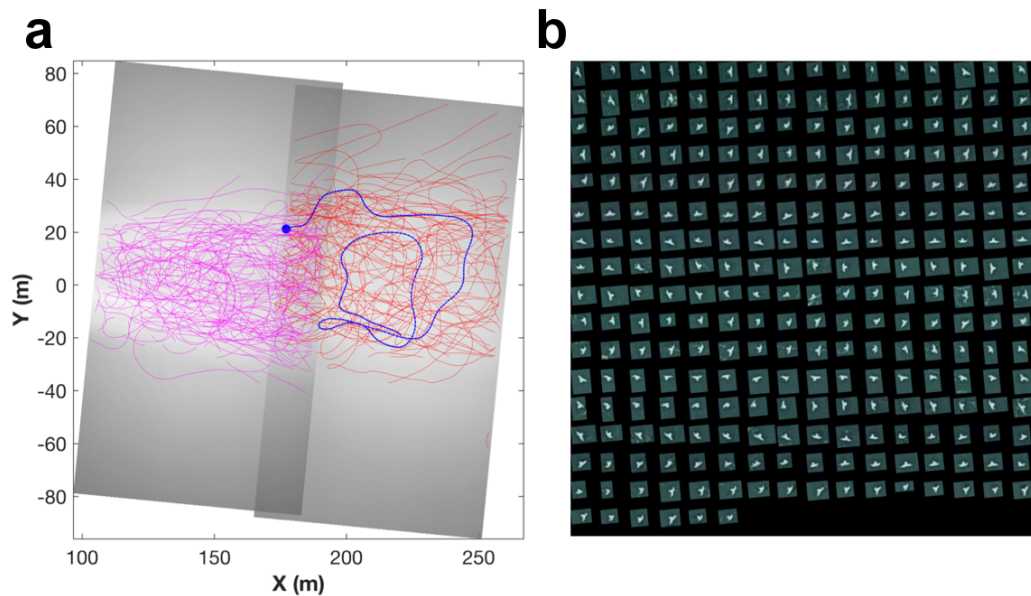
153

154

155

156

157

Fig. 4: Tern flight trajectories recorded during peak flood tide in relation to SeaGen's wake structure. a, Georeferenced trajectories overlaid on time-average video images showing brighter region of foam/suspended material in wake. All trajectories of over 2 s duration are shown from recording periods of 140 s (red, 136 in total) and 125 s (magenta, 196 in total). **b**, Sequence of images of an individual tern as it follows the trajectory indicated in blue in **a** (dot indicates start). Only every fourth image (0.16s time interval) is shown for clarity in row-wise order starting at the top-left of the panel.

Particle flux corresponds with tern foraging patterns Finally, the persistent use of the SeaGen (North) wake by the terns limited to the flood tidal cycle was explored using a hydrodynamic model coupled to an ecological module. Passive particles as a proxy for small prey organisms were released from the Irish Sea, outside the entrance of the Lough at the beginning of a flood tide (Fig. 1b). The flux of incoming potential prey items to SeaGen's flood wake originates 70 min upstream from outside the Lough, corresponding with the rise in tern sightings ~60 min post low water slack.

Discussion

To our knowledge, this is the first study to link indirect physical interactions (a downstream wake) of a renewable energy structure with top predators, highlighting the hitherto overlooked ecological implications of localised physical forcing around man-made structures. While top predator use of anthropogenic structures has been observed elsewhere[44,45], distinct mechanisms may be in place to explain such associations. Namely, 1) natural reefing can increase fish biomass[46], 2) fish can seek

179　flow refuge in the immediate lee of a structure[47] and 3) downstream wake effects can make

180　incoming prey available near the surface through displacement[35,48]. The latter mechanism is

181　currently the least explored in a natural setting despite its importance in high-flow environments,

182　highlighting the relevance of our findings. While natural bathymetric features and associated

183　patterns of shear lines and wake effects have been shown to attract top predators[8], the man-made

184　wake in this study promoted the most persistent and intense foraging aggregations of terns among

185　all wake features investigated. While we did not assess prey vertical distribution, turbulent vertical

186　velocity fluctuations within the wake were greater than 0.5 ms^{-1} (Supplementary Fig. 1), exceeding

187　swimming performance of typical piscivorous tern prey items[13] (e.g. sandeel[49] in the order of 0.2 ms^{-}

188　^{1} or sprat/herring[50] in the order of 0.4 ms^{-1}) and may have the potential to displace prey. Therefore,

189　our future studies will focus on assessing prey distribution and availability within both the inflows

190　and wakes under different tidal states.

191　　　With the intensification of man-made structures in coastal seas, new synergies between

192　these and marine predators are likely. Our findings demonstrate that wake features, predictable in

193　time and space, persistently attract top predators at highly localised scales. We also provide the first

194　empirical evidence that localised hydrodynamic forcing attributable to an anthropogenic structure

195　can present a mechanism to promote a foraging hotspot, where predator aggregations exceed those

196　at adjacent natural wake features. A broader perspective on the ecological implications of offshore

197　installations is critical[23] and requires the identification of such localised physical processes

198　underlying top predator hotspot formation. For seabirds, there is concern that the introduction of

199　renewable energy devices could lead to avoidance, thereby negatively impacting on energy

200　expenditure[51]. Likewise, it has been suggested that hydrodynamic forces around hard structures

201　could modify prey availability, thereby increasing a seabird's rate of energy acquisition[52]. While our

202　findings suggest that terns exploit the flood wake of a device, an overall ecological (population-level)

203　benefit through increased individual energy acquisition can only be determined when accounting for

204　parameters relating to e.g. foraging success, prey profitability and breeding performance[52,53].

205   In the expanding renewable energy sector (e.g. >4000 offshore wind turbines in Europe[54]), monopile

206   foundations similar to the SeaGen design present the most common substructure (66%[54]) and lead

207   to comparable wake vortices[25,27,55]. However, even submerged tidal turbines, and more so arrays,

208   placed in unsteady flows will change the local hydrodynamic regime including wake effects[26,56] and

209   more empirical data are required to predict changes in hydrodynamics and foraging habitat.

210   With SeaGen being decommissioned, its removal will undoubtedly change the foraging

211   aggregations observed here. The decommissioning process, often requiring the complete removal of

212   an aging structure[57], is currently being re-considered globally by evidence of potential ecological

213   benefits through artificial reef effects[58] and increased fish biomass[59,46] if parts remain in the sea.

214   However, there is equal concern about the possible ecological impacts of artificial structures on

215   marine vertebrates[60] and in terms of their benthic footprint[61,62]. Renewable energy installations

216   show some ecological synergies to oil-and gas platforms[61,63,44] and could become an important

217   contributor to the foreseen 'decommissioning crisis'[64] if not addressed in a timely manner.

218   Therefore, when designing the decommissioning removal scope of devices, a case-by-case

219   determination of the ecological benefits or disadvantages of seemingly obsolete installations is

220   required[65].

221

222   ## Methods

223   **Study site** All wake features investigated are situated in the Narrows, a tidal channel linking

224   Strangford Lough, Northern Ireland, UK, with the Irish Sea (Fig. 1). The three sites investigated were

225   1) Walter's Rock (54° 22.992'N, 5° 33.504'W), an island located on the periphery of the main

226   channel, generating local upwelling and shear lines extending both into the channel and the near-

227   shore shallows; 2) SeaGen (54° 22.122'N, 5° 32.766'W), located in the mid-channel and experiences

228   the highest current magnitudes[39] and 3) the Routen Wheel (54° 21.698'N, 5° 32.476'W), turbulent

229   whirlpool structures that are generated from a shallow pinnacle (5 m depth) surrounded by 20 m

230   deep waters. Here, the asymmetrical bathymetry of the channel promotes a more intense

231   turbulence field at the surface during the ebb tide. While all three wake features differ in

232   composition, they all predictably create local zones of extreme turbulent flow structures and tern

233   feeding flocks had been observed at all three features prior to the study. With various tern (*Sterna*

234   *sandvicensis, S. hirundo, S. paradisaea*) colonies located across Strangford Lough, Swan island

235   presents the nearest colony to any of these wake features (Fig. 1). Sandwich terns are most

236   abundant with 776 AONs (Apparently Occupied Nests which equates to the number of breeding

237   pairs), followed by common (340 AONs) and Artic (193 AONs) terns, respectively (pers. comm. Hugh

238   Thurgate, National Trust, Strangford Lough head ranger).

239   **Data collection and analysis** A vantage point study was designed to collect count data of terns over

240   the wake features between 18th July 2018 and 12th August 2018. Vantage points were located on the

241   shore with a 200m-1km distance from each feature and covered an area of ~0.05km² for each site to

242   assess bird numbers associating with each localised wake feature. Observations covered all tidal

243   states over a spring and neap tidal cycle. Using binoculars (Opticron Verano BGA HD and Nikon

244   Monarch 10x42), counts of hovering or diving birds deemed foraging were completed every 2nd/3rd

245   minute for 15min with a 5min rest period to avoid observer fatigue (mean survey period across

246   sites=129min, SD=41min). Number of surveys varied minimally per site, with Walter's Rock (n=9),

247   SeaGen (n=13) and Routen Wheel (n=11) with a total observation time of 23.38 hrs, 25.26 hrs and

248   22.14 hrs, respectively. A general-additive mixed effect model (GAMM) was performed to quantify

249   variances in the probability of encountering terns and the number of terns if encountered among

250   tidal states and locations. A binomial model was used for the probability of encountering terns, and

251   a negative binomial was used for the number of terns if encountered. Location was used as a

252   categorical explanatory variable. Tidal state (hours after high water) was used as a continuous and

253   non-linear explanatory variable. The number of knots was constrained to six to avoid over-fitting.

254   Tidal state was also modelled as an interaction with location to account for differences in patterns

255   among locations. An AR1 structure was used to account for temporal autocorrelation in model

256   residuals within locations. Model parameters were used to predict variations in the probability of

257   encountering terns and the number of terns if encountered across different locations and tidal

258   states. Differences in probabilities and numbers across locations and tidal states were tested for

259   significance ($p < 0.05$) using F-tests. Models were performed in the mgcv packages in R Statistics[66].

260   **Unmanned Aerial Vehicle (UAV) surveys** To record fine-scale foraging behaviour in relation to the

261   wakes, UAV surveys were performed from the nearest accessible shore location to each feature

262   using a DJI Mavic Pro quadcopter recording 4 K video at 25 fps. The UAV was flown manually using

263   the DJI Go v4.0 application. In order to comply with best practices[67] and minimise potential

264   disturbance, the vertical ascent of the UAV was made at 200 m distance from the foraging

265   aggregations and sampling was performed at a height of 120 m above-surface level, as measured by

266   the on-board altimeter. Missions included transects across SeaGen as well as hovering (holding

267   station with a vertically downward-facing camera) over the flood wake of SeaGen to capture seabird

268   flight tracks over time. Surveys reported here were conducted on 11 July 2018 during a flood tidal

269   cycle (07:30 hrs – 08:30 hrs GMT) with a total flight time of 41 minutes. All missions were completed

270   in accordance with local regulations and flown by the same qualified (UK Civil Aviation Authority)

271   pilot. The UAV camera was calibrated in the lab and video sequences post-processed using MATLAB

272   (R2017b; Mathworks). Georeferenced composite panoramic images captured the distribution of

273   terns up-and downstream of SeaGen. Machine learning approaches were used to identify, count and

274   track terns over SeaGen's flood wake. Briefly, moving objects were detected using frame-to-frame

275   differencing, segmentation and then filtered by size to remove sun-glint speckles and large foam

276   patches. Images of potential targets were then passed through a trained "Bag of Features" classifier

277   before using Kalman filters to compile tracks of those targets identified as terns only. The classifier

278   was trained using 806 manually-identified images each of foam and terns, with an average accuracy

279   of 93% when applied to a validation set of 3764 images.

280   **Acoustic Doppler current profiler (ADCP) surveys** Vessel-mounted ADCP transects were performed

281   on 13 Aug 2018 using a pole-mounted (1.15 m depth) RDI Workhorse Monitor broadband ADCP (600

282   kHz) in bottom-tracking mode with a vertical bin size of 1 m. All data was acquired using VMDas

283   software (v. 1.46; RD Instruments, Inc.) and post-processed in WinADCP (v. 1.14; RD Instruments,

284   Inc.). True current velocities were computed by subtraction of the bottom-tracked boat velocity. To

285   quantify the acoustic scattering in the water column as a metric for macro-turbulence[39], volume-

286   backscattering strength (Sv in decibels, dB) was calculated across a maximum of 40 bins from the

287   ADCP's recorded raw echo intensity data using a working version of the sonar equation as originally

288   described in Deines[68] and updated by Mullison[69]. The backscatter equation accounts for two-way

289   transmission loss, time-varying gain, water absorption, and uses an instrument- and beam-specific

290   RSSI scaling factor to convert counts to decibels. This makes it a more robust measure of scattering

291   compared to raw echo intensity which can be more readily extracted from the ADCP. Sv was

292   calculated for each bin along each of the four beams of the ADCP. For each range bin, the maximum

293   of the four beams (Sv_{max}) was taken to create depth profiles of the maximum level of scattering

294   across the water column. In high-flow environments, high values of acoustic scattering are

295   dominated by enhanced surface bubble entrainment and sediment re-suspension[22,41,70].

296   **Hydrodynamic modelling** The Strangford Lough hydrodynamic model developed using MIKE21

297   modelling software (DHI Water and Environment software package: www.dhisoftware.com)[71] was

298   used to simulate particle movement in the Narrows. In short, the model uses a finite volume method

299   by solving a depth averaged shallow water approximation. Full details of the model setup can be

300   found in Kregting[71]. The Strangford Lough model was coupled to a particle tracking module that

301   incorporates advection and dispersion resolved using the Langevin equation. For horizonal

302   movement, in the absence of any dispersion (horizontal or vertical) information, the scaled eddy

303   viscosity was used with the software recommended constant value of 1.0. For the vertical

304   dispersion, a constant dispersion value of 0.01 m^2 per second was used. Changes in flow velocity

305   throughout the water column were calculated based on the bed friction velocity, a parameter

306   calculated directly in the hydrodynamic model. Passive particles as proxy for microscopic or small

307   organisms were released from the Irish Sea at a depth of 10 m, approximately half the water column

308   height (Fig. 1). A trickle release approach was adopted where 200 particles were released every 5

309   min timestep on the flood tide only and the time taken from release to the time taken to reach

310   SeaGen was noted.

311

312   **Data Availability**. The dataset used to generate the main result shown in Figure 2 is available online
313   at https://doi.org/10.6084/m9.figshare.7732514.v1. All other data generated and analysed during
314   the current study are available from the corresponding author on reasonable request.

315

References

317

318   1.   Dafforn, K. A. *et al.* Marine urbanization: An ecological framework for designing
319   multifunctional artificial structures. *Front. Ecol. Environ.* **13,** 82–90 (2015).

320   2.   Pinaud, D. & Weimerskirch, H. Scale-dependent habitat use in a long-ranging central place
321   predator. *J. Anim. Ecol.* **74,** 852–863 (2005).

322   3.   Bertrand, A. *et al.* Broad impacts of fine-scale dynamics on seascape structure from
323   zooplankton to seabirds. *Nat. Commun.* **5,** 1–9 (2014).

324   4.   Abrahms, B. *et al.* Mesoscale activity facilitates energy gain in a top predator. *Proc. R. Soc. B
325   Biol. Sci.* **285,** 20181101 (2018).

326   5.   Miller, P. I., Scales, K. L., Ingram, S. N., Southall, E. J. & Sims, D. W. Basking sharks and
327   oceanographic fronts: quantifying associations in the north-east Atlantic. *Funct. Ecol.* **29,**
328   1099–1109 (2015).

329   6.   Tew Kai, E. *et al.* Top marine predators track Lagrangian coherent structures. *Proc. Natl. Acad.
330   Sci. U. S. A.* **106,** 8245–8250 (2009).

331   7.   Scales, K. L. *et al.* Mesoscale fronts as foraging habitats: composite front mapping reveals
332   oceanographic drivers of habitat use for a pelagic seabird. *J. R. Soc. interface* **11,** 20140679.
333   (2014).

334   8.   Johnston, D. W. & Read, A. J. Flow-field observations of a tidally driven island wake used by
335   marine mammals in the Bay of Fundy, Canada. *Fish. Oceanogr.* **16,** 422–435 (2007).

336   9.   Thorne, L. H. & Read, A. J. Fine-scale biophysical interactions drive prey availability at a
337   migratory stopover site for Phalaropus spp . in the Bay of Fundy , Canada. *Mar. Ecol. Prog.
338   Ser.* **487,** 261–273 (2013).

339   10.   Zamon, J. E. Mixed species aggregations feeding upon herring and sandlance schools in a
340   nearshore archipelago depend on flooding tidal currents. *Mar. Ecol. Prog. Ser.* **261,** 243–255
341   (2003).

342   11.   Braune, B. M. & Gaskin, D. E. Feeding Ecology of Nonbreeding Populations of Larids off Deer
343   Island, New Brunswick. *Auk* **99,** 67–76 (1982).

344   12.   Urmy, S. S. & Warren, J. D. Foraging hotspots of common and roseate terns: the influence of
345   tidal currents, bathymetry, and prey density. *Mar. Ecol. Prog. Ser.* **590,** 227–245 (2018).

346   13.   Cabot, D. & Nisbet, I. *Terns. Collins, London, UK*. (2013).

347   14.   Duffy, D. C. Predator-Prey Interactions between Common Terns and Butterfish. *Ornis Scand.*

348 *(Scandinavian J. Ornithol.* **19,** 160–163 (1988).

349 15. Schwemmer, P., Adler, S., Guse, N., Markones, N. & Garthe, S. Influence of water flow
350   velocity, water depth and colony distance on distribution and foraging patterns of terns in the
351   Wadden Sea. *Fish. Oceanogr.* **18,** 161–172 (2009).

352 16. Boyd, C. *et al.* Predictive modelling of habitat selection by marine predators with respect to
353   the abundance and depth distribution of pelagic prey. *J. Anim. Ecol.* (2015).
354   doi:10.1111/1365-2656.12409

355 17. Ladd, C., Jahncke, J., Hunt, G. L., Coyle, K. O. & Stabeno, P. J. Hydrographic features and
356   seabird foraging in Aleutian Passes. *Fish. Oceanogr.* **14,** 178–195 (2005).

357 18. Stevick, P. *et al.* Trophic relationships and oceanography on and around a small offshore
358   bank. *Mar. Ecol. Prog. Ser.* **363,** 15–28 (2008).

359 19. Waggitt, J. J. *et al.* Combined measurements of prey availability explain habitat selection in
360   foraging seabirds. *Biol. Lett.* **14,** 20180348. (2018).

361 20. Weimerskirch, H. Are seabirds foraging for unpredictable resources? *Deep. Res. Part II Top.*
362   *Stud. Oceanogr.* **54,** 211–223 (2007).

363 21. Hazen, E. L. *et al.* Scales and mechanisms of marine hotspot formation. *Mar. Ecol. Prog. Ser.*
364   **487,** 177–183 (2013).

365 22. Nimmo-Smith, W. A. M., Thorpe, S. A. & Graham, A. Surface effects of bottom-generated
366   turbulence in a shallow tidal sea. *Nature* **400,** 251–254 (1999).

367 23. Shields, M. A. *et al.* Marine renewable energy: The ecological implications of altering the
368   hydrodynamics of the marine environment. *Ocean Coast. Manag.* **54,** 2–9 (2011).

369 24. Fraser, S., Nikora, V., Williamson, B. J. & Scott, B. E. Hydrodynamic Impacts of a Marine
370   Renewable Energy Installation on the Benthic Boundary Layer in a Tidal Channel. *Energy*
371   *Procedia* **125,** 250–259 (2017).

372 25. Floeter, J. *et al.* Pelagic effects of offshore wind farm foundations in the stratified North Sea.
373   *Prog. Oceanogr.* **156,** 154–173 (2017).

374 26. Churchfield, M. J., Li, Y. & Moriarty, P. J. A Large-Eddy Simulation Study of Wake Propagation
375   and Power Production in an Array of Tidal- Current Turbines. *Philos. Trans. R. Soc. A*
376   **371:201204,** (2013).

377 27. Rivier, A., Bennis, A. C., Pinon, G., Magar, V. & Gross, M. Parameterization of wind turbine
378   impacts on hydrodynamics and sediment transport. *Ocean Dyn.* **66,** 1285–1299 (2016).

379 28. Vanhellemont, Q. & Ruddick, K. Turbid wakes associated with offshore wind turbines
380   observed with Landsat 8. *Remote Sens. Environ.* **145,** 105–115 (2014).

381 29. Karman, T. Von. The Fundamentals of the Statistical Theory of Turbulence. *J. Aeronaut. Sci.* **4,**
382   131–138 (1937).

383 30. Creech, A. C. W., Borthwick, A. G. L. & Ingram, D. Effects of support structures in an LES
384   actuator line model of a tidal turbine with contra-rotating rotors. *Energies* **10,** 1–25 (2017).

385 31. Webb, P. W. Entrainment by river chub Nocomis micropogon and smallmouth bass
386   Micropterus dolomieu on cylinders. *J. Exp. Biol.* **291,** 2403–2412 (1998).

387 32. Liao, J. C. The Karman gait: novel body kinematics of rainbow trout swimming in a vortex
388   street. *J. Exp. Biol.* **206,** 1059–1073 (2003).

389   33.   Tritico, H. M. & Cotel, A. J. The effects of turbulent eddies on the stability and critical
390   swimming speed of creek chub (Semotilus atromaculatus). *J. Exp. Biol.* **213,** 2284–2293
391   (2010).

392   34.   Liao, J. C. A review of fish swimming mechanics and behaviour in altered flows. *Philos. Trans.*
393   *R. Soc. Lond. B. Biol. Sci.* **362,** 1973–1993 (2007).

394   35.   Cote, A. J. & Webb, P. W. Living in a turbulent world - A new conceptual framework for the
395   interactions of fish and eddies. *Integr. Comp. Biol.* **55,** 662–672 (2015).

396   36.   Lupandin, A. I. Effect of Flow Turbulence on Swimming Speed of Fish. *Biol. Bull.* **32,** 461–466
397   (2005).

398   37.   Hale, R. & Swearer, S. E. Ecological traps: Current evidence and future directions. *Proc. R. Soc.*
399   *B Biol. Sci.* **283,** 1–8 (2016).

400   38.   Martin, T. G. *et al.* Zero tolerance ecology : improving ecological inference by modelling the
401   source of zero observations. *Ecol. Lett.* **8,** 1235–1246 (2005).

402   39.   Lieber, L., Nimmo-Smith, W. A. M., Waggitt, J. J. & Kregting, L. Fine-scale hydrodynamic
403   metrics underlying predator occupancy patterns in tidal stream environments. *Ecol. Indic.* **94,**
404   397–408 (2018).

405   40.   Lavery, A. C., Chu, D. & Moum, J. N. Measurements of acoustic scattering from zooplankton
406   and oceanic microstructure using a broadband echosounder. *ICES J. Mar. Sci.* **67,** 379–394
407   (2010).

408   41.   Holdaway, G. P., Thorne, P. D., Flatt, D., Jones, S. E. & Prandle, D. Comparison between ADCP
409   and transmissometer measurements of suspended sediment concentration. *Cont. Shelf Res.*
410   **19,** 421–441 (1999).

411   42.   Demer, D. A., Barange, M. & Boyd, A. J. Measurements of three-dimensional fish school
412   velocities with an acoustic Doppler current profiler. *Fish. Res.* **47,** 201–214 (2000).

413   43.   Zedel, L. & Cyr-Racine, F.-Y. Extracting fish and water velocity from Doppler profiler data. *ICES*
414   *J. Mar. Sci.* **66,** 1846–1852 (2009).

415   44.   Russell, D. J. F. *et al.* Marine mammals trace anthropogenic structures at sea. *Curr. Biol.* **24,**
416   R638–R639 (2014).

417   45.   Burke, C. M., Montevecchi, W. A. & Wiese, F. K. Inadequate environmental monitoring
418   around offshore oil and gas platforms on the Grand Bank of Eastern Canada : Are risks to
419   marine birds known? *J. Environ. Manage.* **104,** 121–126 (2012).

420   46.   Claisse, J. T. *et al.* Oil platforms off California are among the most productive marine fish
421   habitats globally. *Proc. Natl. Acad. Sci.* **111,** 15462–15467 (2014).

422   47.   Liao, J. C. A review of fish swimming mechanics and behaviour in altered flows. *Philos. Trans.*
423   *R. Soc. Lond. B. Biol. Sci.* **362,** 1973–1993 (2007).

424   48.   Harvey, B. C. Susceptibility of Young-of-the-Year Fishes to Downstream Displacement by
425   Flooding. *Trans. Am. Fish. Soc.* (1987).

426   49.   Behrens, J. W. & Steffensen, J. F. The effect of hypoxia on behavioural and physiological
427   aspects of lesser sandeel, Ammodytes tobianus (Linnaeus , 1785). *Mar. Biol.* **150,** 1365–1377
428   (2007).

429   50.   Turnpenny, A. W. H. Swimming performance of juvenile sprat, Sprattus sprattus L., and

430   herring, Clupea harengus L., at different salinities. *J. Fish Biol.* **23,** 321–325 (1983).

431 51. Masden, E. A. *et al.* Barriers to movement: Impacts of wind farms on migrating birds. *ICES J.*
432   *Mar. Sci.* **66,** 746–753 (2009).

433 52. Langton, R., Davies, I. M. & Scott, B. E. Seabird conservation and tidal stream and wave power
434   generation: Information needs for predicting and managing potential impacts. *Mar. Policy* **35,**
435   623–630 (2011).

436 53. Reynolds, S. J. *et al.* Long - term dietary shift and population decline of a pelagic seabird — A
437   health check on the tropical Atlantic ? *Glob. Chang. Biol.* **00,** 1–12 (2019).

438 54. Selot, F., Fraile, D. & Brindley, G. *Offshore Wind in Europe -Key trends and statistics 2018.*
439   *Wind Europe* (2018).

440 55. Grashorn, S. & Stanev, E. V. Kármán vortex and turbulent wake generation by wind park piles.
441   *Ocean Dyn.* **66,** 1543–1557 (2016).

442 56. Ouro, P., Runge, S., Luo, Q. & Stoesser, T. Three-dimensionality of the wake recovery behind a
443   vertical axis turbine. *Renew. Energy* **133,** 1066–1077 (2019).

444 57. Hamzah, B. A. International rules on decommissioning of offshore installations: Some
445   observations. *Mar. Policy* **27,** 339–348 (2003).

446 58. Bell, N. & Smith, J. Coral growing on North Sea oil rigs. *Nature* **402,** 601 (1999).

447 59. Macreadie, P. I., Fowler, A. M. & Booth, D. J. Rigs-to-reefs: Will the deep sea benefit from
448   artificial habitat? *Front. Ecol. Environ.* **9,** 455–461 (2011).

449 60. Fox, C. J., Benjamins, S., Masden, E. A. & Miller, R. Challenges and opportunities in monitoring
450   the impacts of tidal-stream energy devices on marine vertebrates. *Renew. Sustain. Energy*
451   *Rev.* **81,** 1926–1938 (2018).

452 61. Miller, R. G. *et al.* Marine renewable energy development: Assessing the Benthic Footprint at
453   multiple scales. *Front. Ecol. Environ.* **11,** 433–440 (2013).

454 62. Heery, E. C. *et al.* Journal of Experimental Marine Biology and Ecology Identifying the
455   consequences of ocean sprawl for sedimentary habitats. *J. Exp. Mar. Bio. Ecol.* **492,** 31–48
456   (2017).

457 63. Inger, R. *et al.* Marine renewable energy: Potential benefits to biodiversity? An urgent call for
458   research. *J. Appl. Ecol.* **46,** 1145–1153 (2009).

459 64. Fowler, A. M., Macreadie, P. I., Jones, D. O. B. & Booth, D. J. A multi-criteria decision
460   approach to decommissioning of offshore oil and gas infrastructure. *Ocean Coast. Manag.* **87,**
461   20–29 (2014).

462 65. Fowler, A. M. *et al.* Environmental benefits of leaving offshore infrastructure in the ocean.
463   *Front. Ecol. Environ.* 571–578 (2018). doi:10.1002/fee.1827

464 66. Wood, S. N. Generalized Additive Models: An Introduction with R (2nd edition). in *Chapman*
465   *and Hall/CRC Press* (2017). doi:10.1111/j.1541-0420.2007.00905_3.x

466 67. Hodgson, J. C. & Koh, L. P. Best practice for minimising unmanned aerial vehicle disturbance
467   to wildlife in biological field research. *Curr. Biol.* **26,** R404–R405 (2016).

468 68. Deines, K. L. Backscatter estimation using Broadband acoustic Doppler current profilers. *Proc.*
469   *IEEE Sixth Work. Conf. Curr. Meas. (Cat. No.99CH36331)* 1–5 (1999).
470   doi:10.1109/CCM.1999.755249

471 69. Mullison, J. Backscatter Estimation Using Broadband Acoustic Doppler Current Profilers -
472   Updated. *Appl. Note, Teledyne RD Instruments* **FSA-031 cr,** 8–13 (2017).

473 70. Lavery, A. C., Geyer, W. R. & Scully, M. E. Broadband acoustic quantification of stratified
474   turbulence. *J. Acoust. Soc. Am.* **134,** 40–54 (2013).

475 71. Kregting, L. & Elsäßer, B. A Hydrodynamic Modelling Framework for Strangford Lough Part 1:
476   Tidal Model. *J. Mar. Sci. Eng.* **2,** 46–65 (2014).

477

487

488 **Author contributions**. L.L. conceived the ideas and all authors designed aspects of the methodology.
489 L.K. managed the project. L.L. and J.J.W. collected the vantage point data; W.A.M.N.S. collected the
490 UAV data (CAA-approved pilot) and L.L. collected the ADCP data. All authors performed analysis and
491 interpreted the results. L.L. drafted the manuscript. All authors contributed critically to the drafts
492 and gave final approval for publication.

493

494 **Competing interests.** The authors declare no competing interests.

495
496
497
498

499 **Figure Legends**

500

501 **Fig. 1:** Location of wake features in the Narrows tidal channel situated in Strangford Lough, Northern
502 Ireland, UK. **a**, Overview map showing the study area within the Narrows, highlighted by a red box.
503 **b**, Location of wake features in the Narrows. c-e, Insets showing the turbulent structures associated
504 with each wake feature. Note: particle release site indicates the release of passive particles (as a
505 proxy for prey organisms) from the Irish Sea during flood tide within a hydrodynamic model.

506

507 **Fig. 2:** Tern counts over tidal state at each wake feature. **a** & **b**, Mean ±SE variations in the predicted
508 probability of encountering terns and the number of terns if encountered per minute across tidal
509 states around SeaGen North and South (**a**), the Routen Wheel and Walter's Rock (**b**) wake features,
510 respectively. Crosses indicate the recorded number of terns if encountered binned into periods
511 representing eight different states (1hr 20min) of the ebb-flood cycle. HT= High tide, LT=Low tide. c,
512 Mean ±SE variations in the predicted probability of encountering terns and the number of terns if
513 encountered per minute across tidal states and locations. Tidal states represent peak current speeds
514 in ebb and flood directions. All predictions (**a-c**) were made using model parameters from a general-
515 additive mixed effect model (GAMM) with significance in both probabilities and numbers across tidal
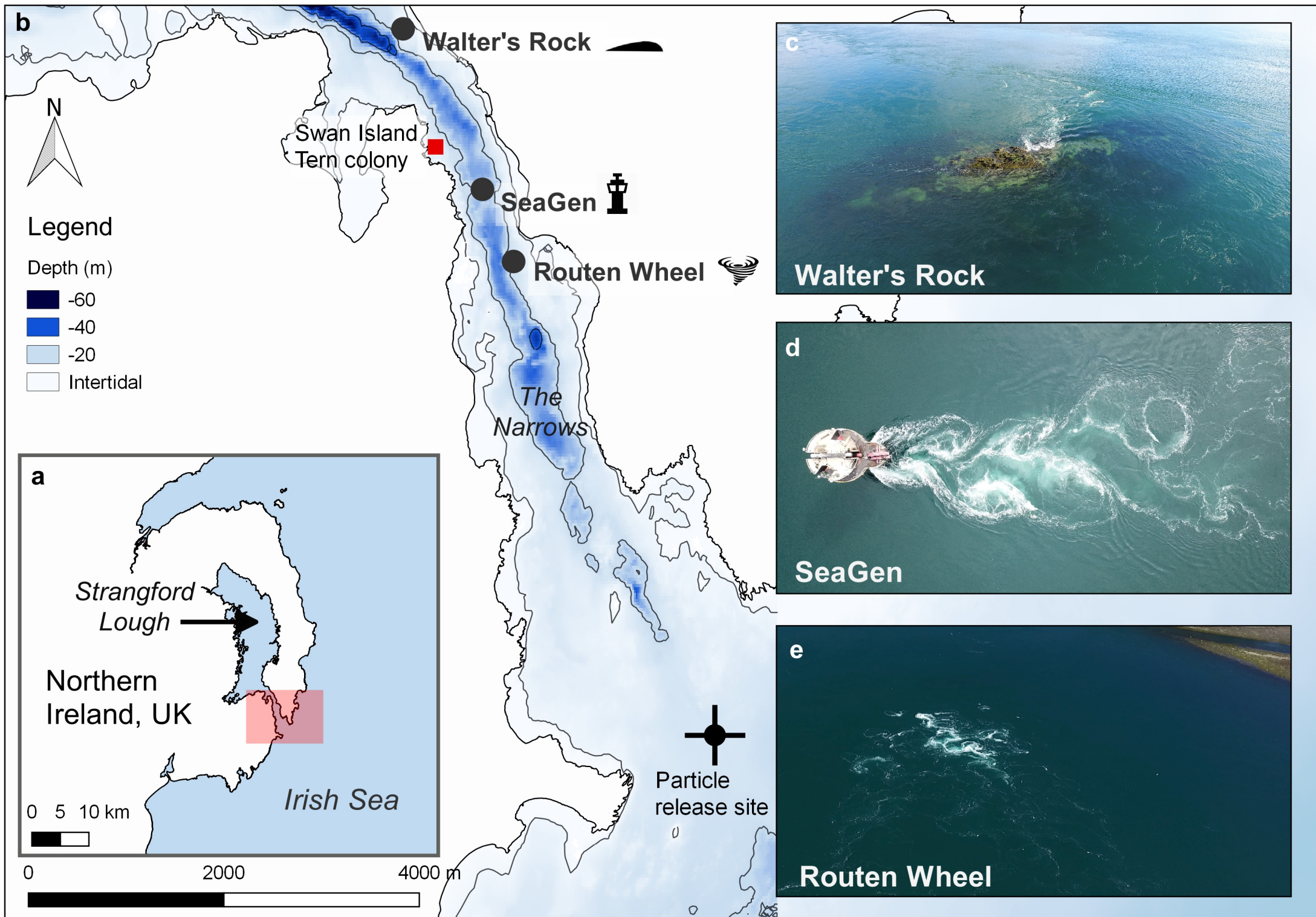516 states shown in Table 1.

517

Fig. 3: Tern distribution during peak flood tide in relation to SeaGen's wake structure. **a,** Georeferenced composite panoramic image from UAV transect survey with terns identified (yellow circles – one enlarged for clarity). The orientation of the x-axis is 349 degrees. Magenta and yellow boxes indicate tracking regions shown in Figure 4. **b-c,** Horizontal velocity magnitude (ms^{-1}) profile from the southern (cyan) and northern (green) ADCP transect, respectively. **d-e,** Maximum acoustic backscatter (dB re $1m^{-1}$) profile from the southern and northern ADCP transect, respectively. The North transects show a clear water column velocity deficit (**c**) and backscatter (an indicator for macro-turbulence) signature (**e**) in the area of the flood wake (Y=-20–20m).
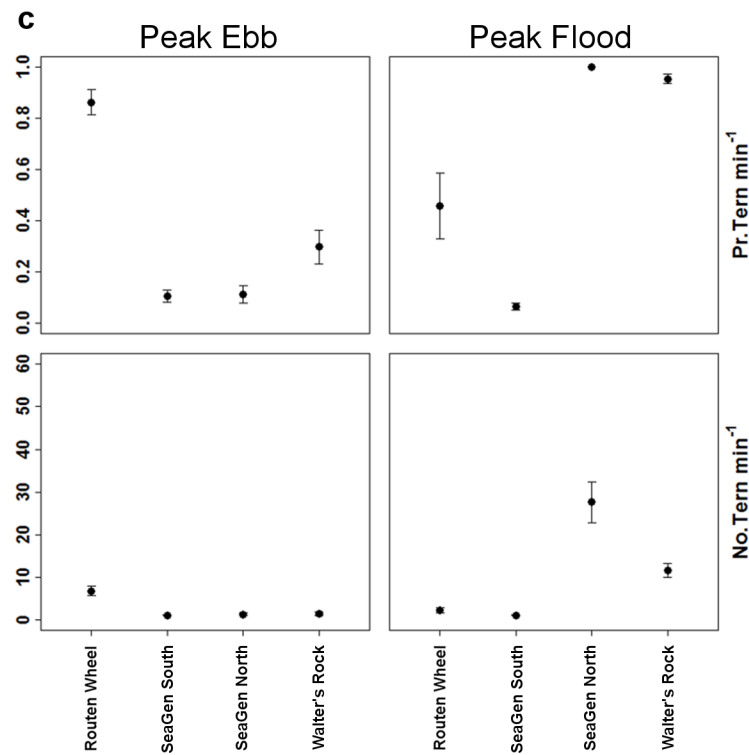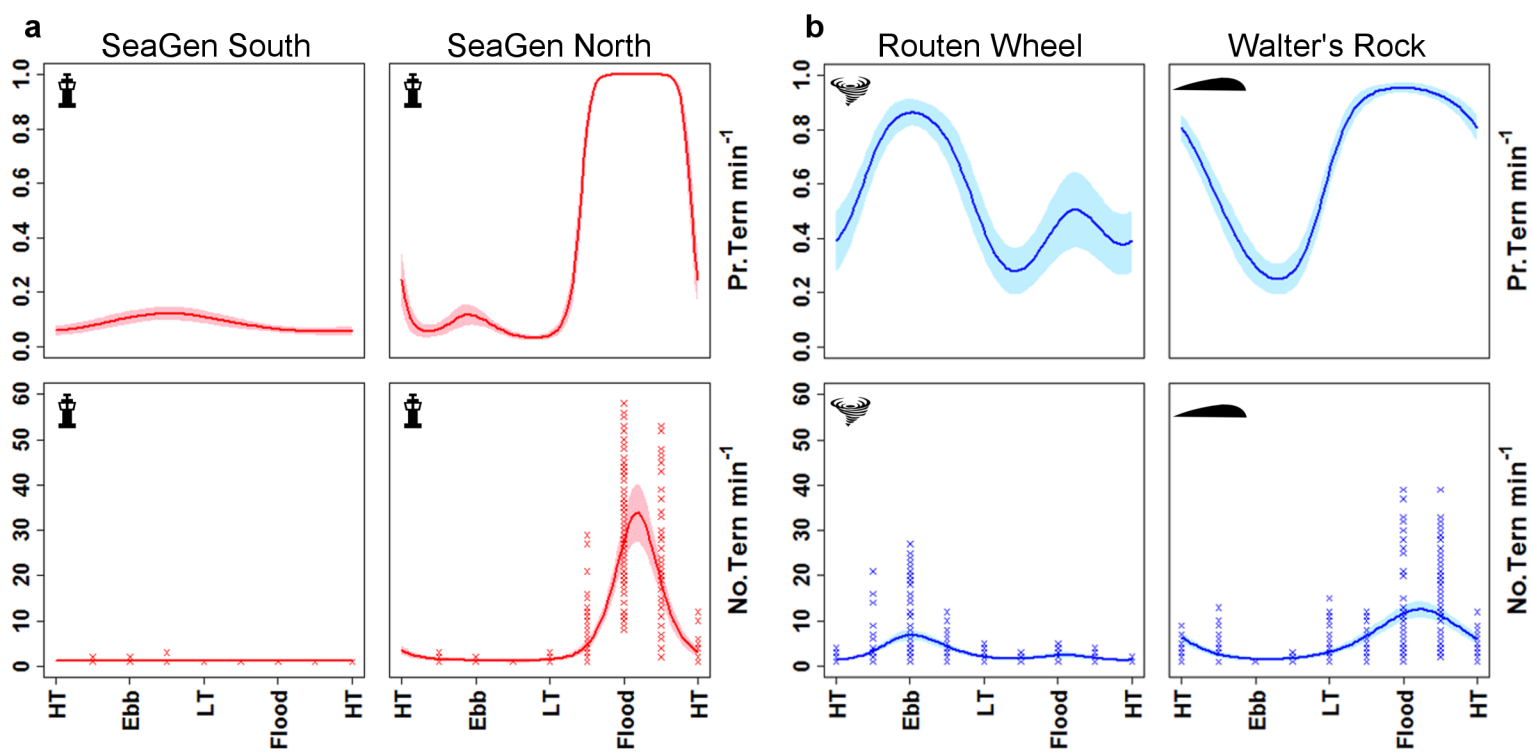
Fig. 4: Tern flight trajectories recorded during peak flood tide in relation to SeaGen's wake structure. **a,** Georeferenced trajectories overlaid on time-average video images showing brighter region of foam/suspended material in wake. All trajectories of over 2 s duration are shown from recording periods of 140 s (red, 136 in total) and 125 s (magenta, 196 in total). **b,** Sequence of images of an individual tern as it follows the trajectory indicated in blue in a (dot indicates start). Only every fourth image (0.16s time interval) is shown for clarity in row-wise order starting at the top-left of the panel.
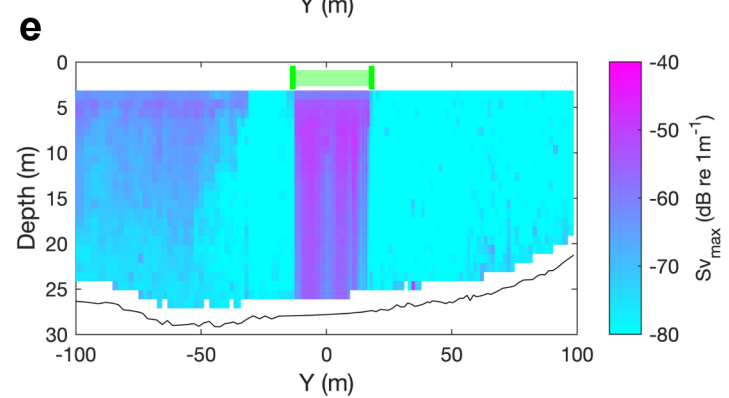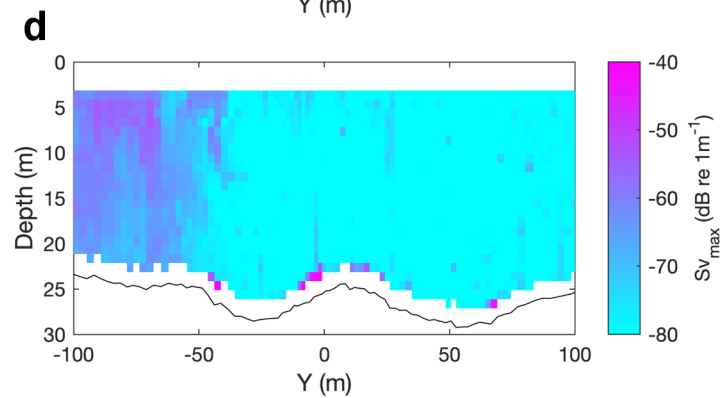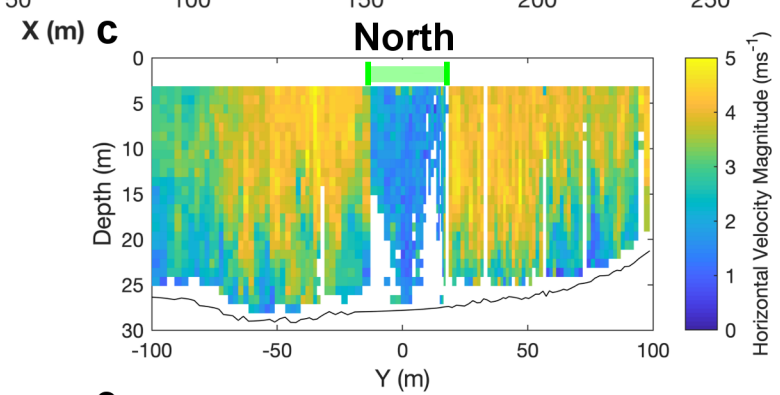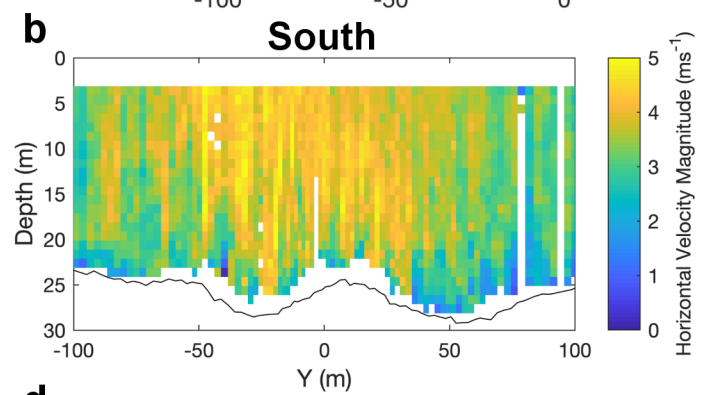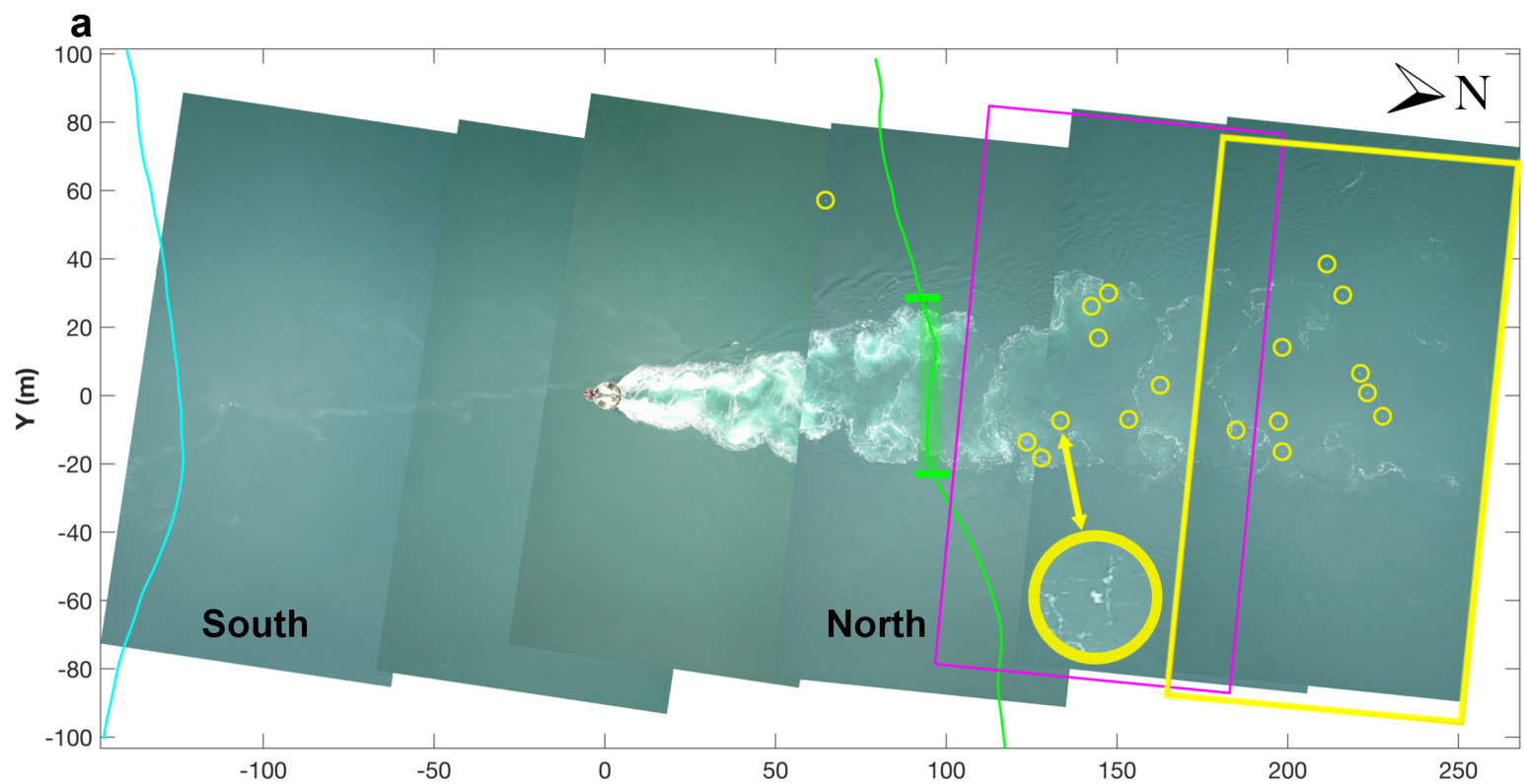
Table

Table 1: General-additive mixed effect model (GAMM) outputs with significance in both probabilities and numbers of terns among sites and within sites across tides.
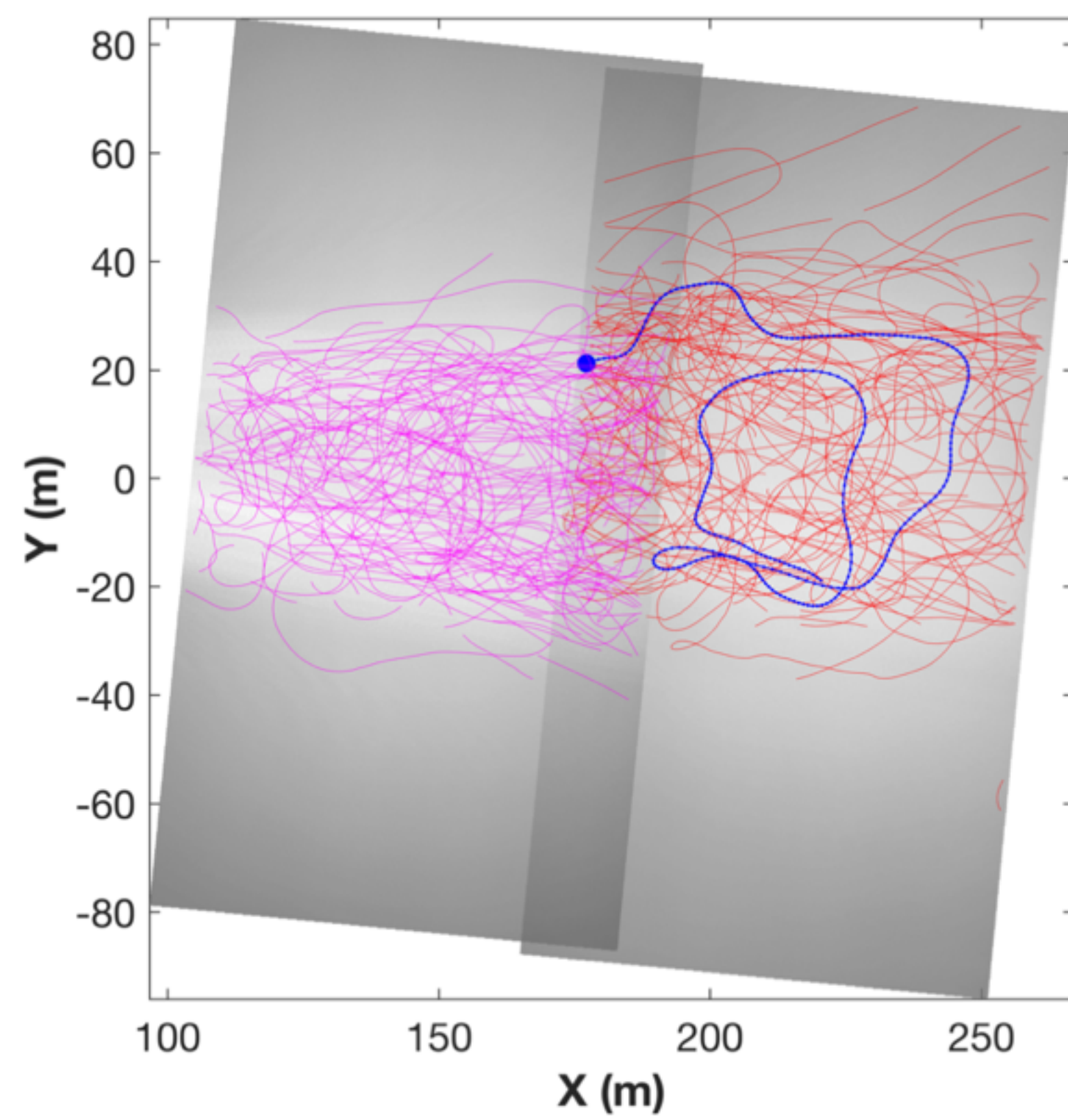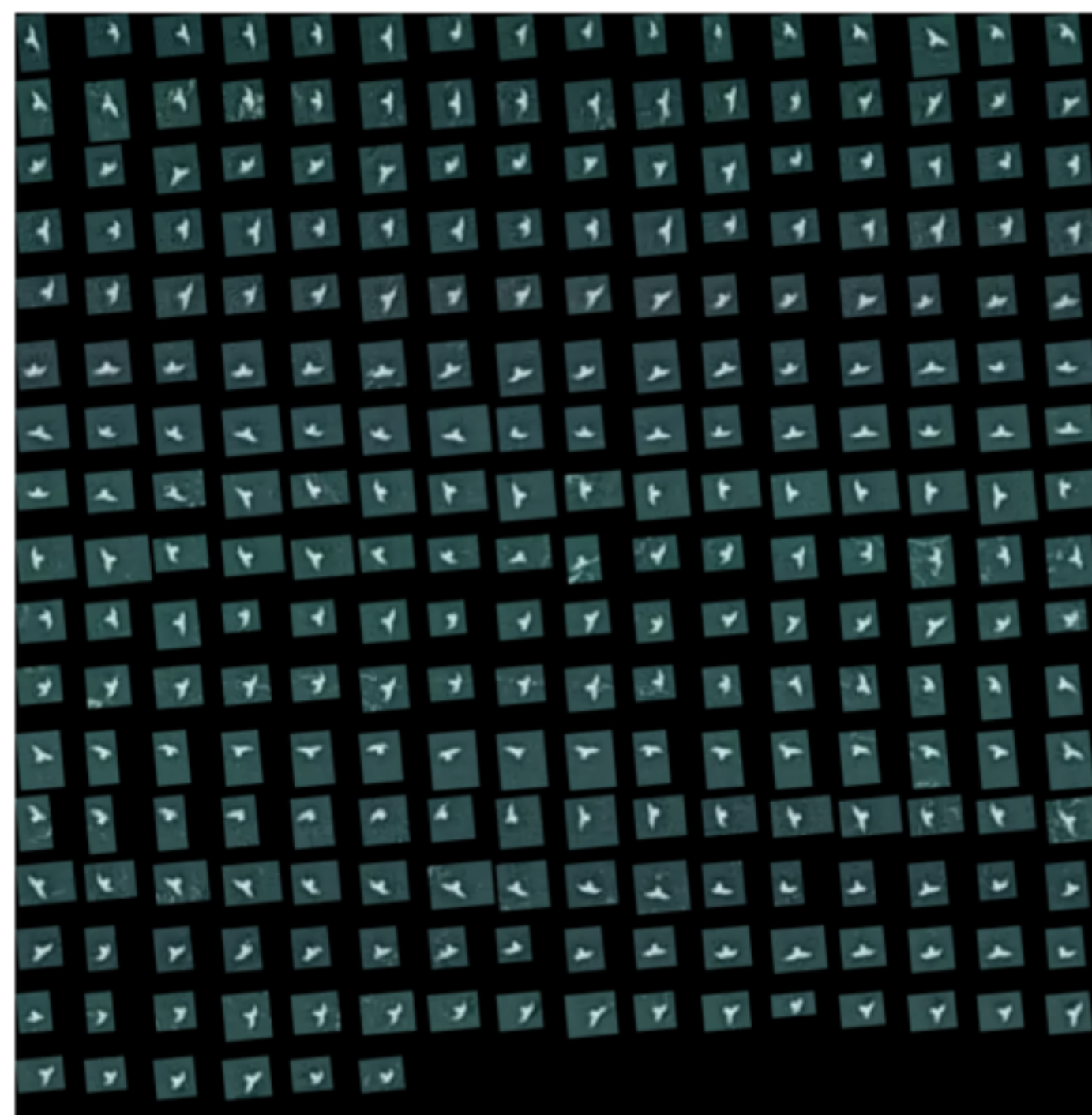
Probability of encountering terns per minute		
Among Sites	$F_{(3,1770)}$ = **109.8**	**p < 0.01**
Across tides in SeaGen North	$F_{(4,1769)}$ = 308.41	p < 0.01
Across tides in SeaGen South	$F_{(4,1769)}$ = 1.60	p = 0.02
Across tides in Routen Wheel	$F_{(4,1769)}$ = 5.64	p < 0.01
Across tides in Walter's Rock	$F_{(4,1769)}$ = 17.55	p < 0.01
Number of terns per minute if encountered		
Among Sites	$F_{(3,789)}$ = **33.69**	**p < 0.01**
Across tides in SeaGen North	$F_{(4,788)}$ = 34.28	p < 0.01
Across tides in SeaGen South	$F_{(4,788)}$ = 0.00	p = 0.88
Across tides in Routen Wheel	$F_{(4,788)}$ = 10.28	p < 0.01
Across tides in Walter's Rock	$F_{(4,788)}$ = 13.51	p < 0.01

b

Walter's Rock

Swan Island
Tern colony

SeaGen

Routen Wheel

The Narrows

Particle release site

Legend

Depth (m)

-60
-40
-20
Intertidal

N

a

Strangford Lough

Northern Ireland, UK

Irish Sea

0 5 10 km

0   2000   4000 m

c Walter's Rock

d SeaGen

e Routen Wheel

a

SeaGen South   SeaGen North

Pr.Tern min⁻¹

No.Tern min⁻¹

b

Routen Wheel   Walter's Rock

Pr.Tern min⁻¹

No.Tern min⁻¹

c

Peak Ebb   Peak Flood

Pr.Tern min⁻¹

No.Tern min⁻¹

Table 1: General-additive mixed effect model (GAMM) outputs with significance in both probabilities and numbers of terns among sites and within sites across tides.

Probability of encountering terns per minute		
Among Sites	$F_{(3,1770)}$ = **109.8**	**p < 0.01**
Across tides in SeaGen North	$F_{(4,1769)}$ = 308.41	p < 0.01
Across tides in SeaGen South	$F_{(4,1769)}$ = 1.60	p = 0.02
Across tides in Routen Wheel	$F_{(4,1769)}$ = 5.64	p < 0.01
Across tides in Walter's Rock	$F_{(4,1769)}$ = 17.55	p < 0.01
Number of terns per minute if encountered		
Among Sites	$F_{(3,789)}$ = **33.69**	**p < 0.01**
Across tides in SeaGen North	$F_{(4,788)}$ = 34.28	p < 0.01
Across tides in SeaGen South	$F_{(4,788)}$ = 0.00	p = 0.88
Across tides in Routen Wheel	$F_{(4,788)}$ = 10.28	p < 0.01
Across tides in Walter's Rock	$F_{(4,788)}$ = 13.51	p < 0.01